TWO ZINC-RICH CHIMNEYS FROM THE PLUME SITE, SOUTHERN JUAN DE FUCA RIDGE

SUZANNE PARADIS

Ottawa–Carleton Geoscience Centre, Department of Earth Sciences, Carleton University, Ottawa, Ontario K1S 5B6

IAN R. JONASSON, GINA M. LE CHEMINANT

Geological Survey of Canada, 601 Booth Street, Ottawa, Ontario, K1A 0E8

DAVID H. WATKINSON

Ottawa–Carleton Geoscience Centre, Department of Earth Sciences, Carleton University, Ottawa, Ontario K1S 5B6

ABSTRACT

Two structurally intact Zn-rich chimneys were collected by the submersible ALVIN from the Plume Site hydrothermal vent, southern Juan de Fuca Ridge. The chimneys display four mineralogically distinct, axially concentric zones A, B, C, D; the outermost zone is A and innermost zone is D. Zone A is highly porous and consists predominantly of fine-grained dendritic sphalerite with minor pyrite and marcasite. Zone B is composed of linked aggregates of dendritic and colloform sphalerite with anhydrite, barite, and amorphous silica that fill cavities. Zone C consists of massive aggregates of sphalerite–wurtzite with minor pyrite and chalcopyrite. Zone D is composed of vuggy, porous aggregates of coarse-grained colloform sphalerite with minor wurtzite, chalcopyrite, isocubanite, pyrite, pyrrhotite and marcasite. The chimneys grew initially by rapid deposition of fine-grained dendritic sphalerite under relatively low-temperature conditions. Subsequent deposition of Zn and Fe sulfides thickened the chimney walls, reduced porosity, and created a physical barrier that inhibited mixing of seawater and hydrothermal fluid within the chimneys. Increase of temperature of the venting fluids led to inward growth of Cu and Fe sulfides within the conduits.

Keywords: Zn-rich chimneys, hydrothermal vent, Juan de Fuca Ridge, Plume Site, sulfides, sulfates, sphalerite.

SOMMAIRE

Nous avons échantillonné deux cheminées zincifères intactes au site de l'évent Plume, dans le secteur sud de la crête Juan de Fuca, au moyen du sous-marin ALVIN. Les cheminées comportent quatre zones minéralogiques distinctes, disposées de façon concentrique. La zone externe (A), en contact avec l'eau de mer, est très poreuse, et contient surtout de la sphalérite dendritique et de rares cristaux de pyrite et de marcasite. La zone B contient un agrégat poreux de sphalérite colloforme et dendritique, avec anhydrite, barytine, et silice amorphe dans les cavités. La zone C comporte un amas massif de sphalérite + wurtzite et une quantité mineure de pyrite et de chalcopyrite. La zone D, partie interne, est faite principalement de sphalérite colloforme, et d'une quantité moindre de wurtzite, chalcopyrite, isocubanite, pyrrhotite, pyrite et marcasite. Les cheminées ont eu une croissance initiale rapide par précipitation de sphalérite dendritique à basse température. Par la suite, la déposition de sulfures de zinc et de fer a épaissi les parois des cheminées, isolant ainsi le fluide hydrothermal de l'eau de mer. Une augmentation de la température à l'intérieur de la cheminée a favorisé la croissance centripète des sulfures de cuivre et de fer.

Mots-clés: cheminées zincifères, évent hydrothermal, crête Juan de Fuca, site Plume, sulfures, sulfates, sphalérite.

INTRODUCTION

Active hydrothermal sites on the southern Juan de Fuca Ridge (USGS Juan de Fuca Study Group 1986, Normark *et al.* 1987) were re-investigated in September 1984 by a U.S. Geological Survey expedition using the submersible ALVIN. At these sites, hydrothermal vents expel high-temperature fluids from which sulfide minerals have precipitated, forming isolated chimney-like edifices several meters high on basaltic rocks of the ridge crest (Koski *et al.* 1982, 1984, Normark *et al.* 1983). Two intact Zn-rich chimneys were sampled from the Plume Site (44°38.6′ N, 130°22.4′ W) of the axial valley of the southern Juan de Fuca Ridge (Figs. 1, 2, 3). This paper describes and discusses mineralogy, textural relationships and chemical variations within the two chimneys, and interprets these features in terms of a model for chimney growth.

METHODS

Minerals were identified using transmitted and reflected light microscopy, quantitative electron-microprobe analyses, and X-ray diffraction studies. Sulfide minerals in the two chimneys were analyzed using a CAMECA electron microprobe equipped with wavelength-dispersion and energy-dispersion systems. Analyses for Cu, Fe, Zn, Cd, Mn, Ag and S were performed on the WDS, using natural or synthetic sulfide and pure metal standards at 20 kV accelerating voltage with a regulated beam current of 30 nA.

GEOLOGICAL SETTING

The Juan de Fuca Ridge is a 500-km section of the mid-ocean rift system situated close to the continental margin of western North America. The study
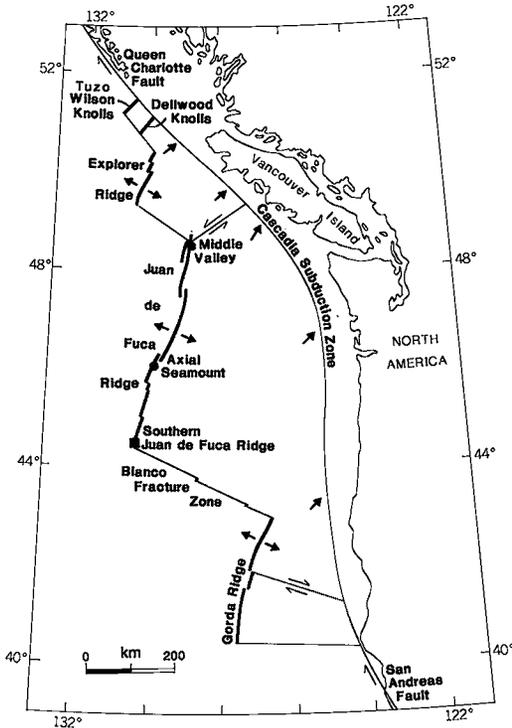
FIG. 1. Location of the Juan de Fuca Ridge and other ridge segments in the northeastern Pacific Ocean.
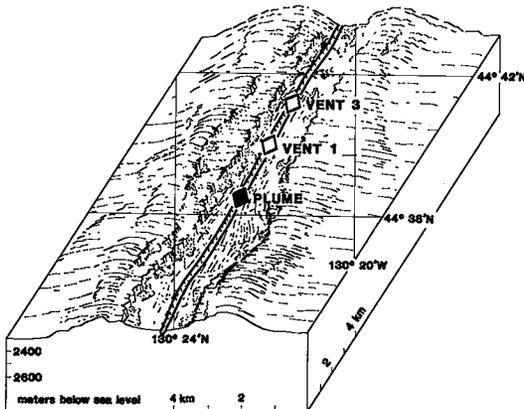
FIG. 2. Physiographic sketch of the Plume Site, Vent 1, and Vent 3 (from Normark et al. 1987).

area is in the southernmost segment of the ridge, 15–20 km north of its intersection with the Blanco Fracture Zone (Fig. 1). This ridge segment has a moderate, half-spreading rate of 3 cm per year (Atwater 1970) and is characterized by a smooth, flat, 1-km wide axial valley enclosed by steep, symmetrical, val-

ley walls and ridges (Normark et al. 1982). The valley floor is made up largely of thin, flat lobate and sheet flows of basaltic pahoehoe lava (Koski et al. 1982, 1984, Normark et al. 1984). Sediment cover is minimal in the southernmost segment of the ridge, but attains 300 m in thickness in the north end at Middle Valley (Davis et al. 1987). Pillow lavas are scarce on the valley floor, but are dominant in the valley walls (Lichtman et al. 1983).

In the study area, the rift axis is characterized by a linear, low-relief (100 m) valley that is bisected by a narrow cleft (Kappel & Normark 1987). A smooth lava plain of ferrobasalt composition (Dixon et al. 1986) forms the valley floor and is broken by numerous collapse pits, especially adjacent to the central cleft (Normark et al. 1987). All known hydrothermal vent sites are located in the cleft. Extensive hydrothermal activity was reported at three sites, viz., Plume Site, Vent 1, and Vent 3 (Fig. 2) which strike over a distance of 5.5 km (USGS Juan de Fuca Study Group 1986).

The two sulfide-rich chimneys described in the present paper were collected in 1984 at the Plume Site. There, hydrothermal sediment is spread for 500 m along the east wall of the cleft, but only two locations show active hydrothermal discharge from chimneys. Elsewhere, shimmering warm waters emanate from many places along the wall. The largest group of spires and chimneys is about 25 m across and is surrounded by an aureole of fluffy yellow sediment consisting of flocs of amorphous Fe oxide, silica, and bacterial filaments (Normark et al. 1987). The sulfides are associated with glassy sheeted lava flows that show little evidence of palagonitization and are probably less than a few hundred years old (Normark et al. 1983). The relative youth of the deposits is supported by a paucity of sulfide rubble around the deposits (USGS Juan de Fuca Study Group 1986) and by the absence of non-specific vent animals at the Plume Site (Tunnicliffe & Fontaine 1987).

The two chimneys are designated ALV-1461-4R and ALV-1462-2R, respectively, (Normark et al. 1987) and are located 25 m apart. Although both were inactive at the time of sampling, active venting was taking place at two sites, one within 10 m of chimney ALV-1462-2R and the other about 15 m from chimney ALV-1461-4R (Fig. 3).

PETROGRAPHY

Chimneys ALV-1461-4R and ALV-1462-2R were cut longitudinally; one half of each was used for the present study, and the other is retained by the USGS Juan de Fuca Study Group at Menlo Park, CA. Each specimen is approximately 15 to 18 cm long and 5 to 6 cm wide. The half-section of ALV-1461-4R was cut into adjoining polished thin sections (7.5 × 5 cm), as shown in Figure 4, to permit mineralogi-

cal investigation of the entire cut face. The half-section of ALV-1462-2R was quartered and one part (left, Fig. 5) was used to prepare adjoining polished thin sections as shown in Figures 5 and 6. A full section cut across the base of ALV-1461-4R was the subject of a detailed S isotopic study by Shanks & Seyfried (1987).

Exterior surfaces of the chimneys display grey, white, orange, and reddish ochre colors, and consist of thin veneers (<1 mm) of Fe oxides and white silica crust intergrown with the remains of adhering vent animals. Sample porosity, which ranges from 5% to 30%, is due to small voids, cavities, and aligned pipe-like structures that are interpreted as sectioned portions of discontinuous and tortuous fluid conduits (e.g., Fig. 5). These crudely elongate or prolate cavities are not abandoned worm tubes; they do not contain the characteristic flaky amorphous silica layer in the inner wall, as described for worm tubes by Koski et al. (1984). Instead, they are interpreted as remnants of fluid conduits through which hot, metal-laden solutions circulated before venting. Because of the similarity of the two half-chimney sections (ALV-1462-2R and ALV-1461-4R), they are described together in the following paragraphs.

The massive sulfide assemblage of each chimney is composed of porous crystallized aggregates of Zn sulfides, smaller amounts of Cu and Fe sulfides, and some sulfates and silicates. Sulfide minerals consist mainly of aggregates of sphalerite–wurtzite with minor pyrite, chalcopyrite, pyrrhotite, isocubanite, and marcasite. The non-sulfide phases are amorphous silica, Fe silicates, barite, and anhydrite which mainly line and infill cavities that occur within dendritic and colloform growth structures in sphalerite.

The chimneys display four mineralogically distinct, axially concentric zones designated as A, B, C and D (Figs. 4–6). The chimney exteriors (zones A and B) consist of light-colored porous aggregates of Zn sulfides, with minor sulfates and silicates, and disseminations of Fe sulfides. The inner chimney walls (zones C and D) consist of dark grey sulfides of Zn, Cu and Fe that are vuggy and relatively unoxidized. Overall, the chimney exteriors are sulfate- and Zn-rich whereas interiors are sulfate-poor and Zn–Cu-rich.

In detail, the outermost few mm of the outer wall (zone A) are highly porous and are composed of dendritic aggregates of fine-grained sphalerite and minor disseminated pyrite and marcasite bordering the sphalerite (Fig. 7a). The dendritic structures, formed by tiny sphalerite euhedra, extend radially outward within the chimney walls. Anhydrite and barite are uncommon, although some relict blades may indicate that they were originally more widespread. The interior of the outer wall (zone B) consists of linked aggregates of colloform and euhedral sphalerite; anhydrite or barite crystals occur in cavities
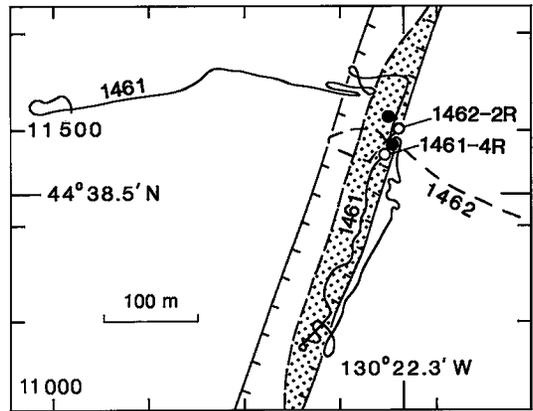
FIG. 3. Location of the Plume Vent Site, southern Juan de Fuca Ridge, showing ALVIN dive tracks 1461 and 1462 sample locations (o) and active vents (•) from USGS Juan de Fuca Study Group (1986). The hachured lines represent the central axial cleft and the stipple outlines area of hydrothermal sedimentation.

(Figs. 7b, c). Pyrite and marcasite are both intimately intergrown with dendritic, colloform sphalerite that seems to have nucleated in pores within marcasite (Fig. 7d); chalcopyrite is rare. Amorphous silica is present in zones A and B. The outer wall of the interior (zone C) is composed of nearly massive aggregates of sphalerite–wurtzite with minor disseminated chalcopyrite and pyrite cubes (Figs. 7e, f). The inner wall of the chimney (zone D) consists of vuggy, porous aggregates of coarser, dark grey sulfides, mostly sphalerite with minor chalcopyrite, wurtzite, isocubanite, pyrrhotite, marcasite, pyrite, and silica. An overall increase in the grain size (<0.02 to 1 mm) of Zn sulfide minerals from the outer to the interior of the chimney is coincident with the above mineralogical trends. Vertically, the interior of chimney ALV-1462-2R is dominated by granular sphalerite in its lower half, and by sphalerite–wurtzite in its upper half. No specific mineralogical and grain-size vertical variations were observed in chimney ALV-1461-4R.

MINERALOGY

Mineral characteristics and modal abundances in the samples are summarized in Tables 1 and 2.

Sphalerite, the most abundant sulfide, accounts for up to 95% of the sulfide content of the chimney sections. Typical textures are: 1) dendritic aggregates of fine-grained sphalerite (zones A and B; Fig. 7a); 2) massive aggregates of subhedral to euhedral sphalerite crystals (zone C; Figs. 7e,f, 8e,f); and 3) coarse-grained colloform sphalerite with delicate growth layers (zone D; Figs. 8a,b,c,d). Wurtzite is

MASSIVE SULFIDE SAMPLE ALV-1461-4R
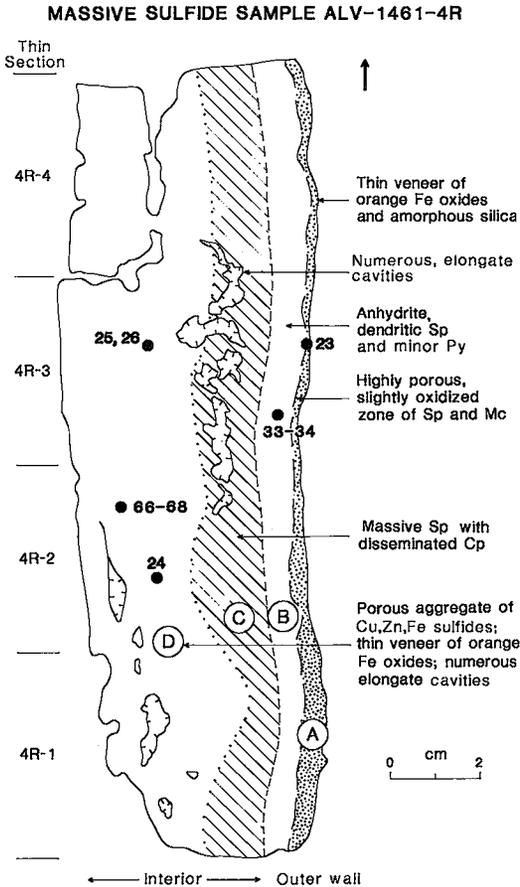
FIG. 4. Sketch of longitudinal section of sample ALV-1461-4R from the Juan de Fuca Ridge. A to D correspond to zones discussed in the text. Numbered points are keyed to microprobe analyses in Table 4. Arrow indicates top of sample. Abbreviations: Sp sphalerite, Cp chalcopyrite, Po pyrrhotite, Py pyrite, Anh anhydrite, and Mc marcasite.

inferred from hexagonal crystal outlines commonly seen in thin section (Fig. 9e), and although XRD data confirm that wurtzite coexists with sphalerite in many parts of these chimneys, the proportions of wurtzite and sphalerite are largely unknown.

Pyrrhotite commonly occurs within zone D of the chimney walls as tabular crystals less than 0.7 mm long (Fig. 9b). Pyrrhotite coexists with chalcopyrite within interstices that remain following precipitation of colloform sphalerite (Figs. 9a,c). Pyrrhotite also occurs as very small laths (0.02 mm long) disseminated in silica gangue or associated with granular sphalerite (Fig. 9d). The former presence of pyrrhotite in outer zones (A, B) is inferred from tabular pseudomorphs now composed of amorphous silica and sphalerite (Fig. 11e).

Isocubanite is cubic cubanite $CuFe_2S_3$ (Oudin & Constantinou 1984). It corresponds chemically to "intermediate solid solution" in the Cu–Fe–S system studied by Kojima & Sugaki (1985), Wiggins & Craig (1980), and Mukaiyama & Isawa (1970). In Plume Site samples, isocubanite is rare and mainly occurs as anhedral cores in euhedral Zn sulfide in chimney zone D (Figs. 9e,f). Although isocubanite is similar to pyrrhotite in reflected light, fine exsolution-like lamellae (1μm or so) of slightly Fe-enriched chalcopyrite are always present within isocubanite cores (Davis *et al.* 1987, Koski *et al.* 1984). These lamellae may result from the rapid-cooling breakdown of an initial phase rich in Zn, Cu, Fe and S to a wurtzite + isocubanite + chalcopyrite + pyrrhotite assemblage (Kojima & Sugaki 1985, Oudin 1983a, Mukaiyama & Isawa 1970). Alternatively, chalcopyrite lamellae could be exsolved from the high-temperature isocubanite phase during the waning phases of hydrothermal activity, in which case the chalcopyrite would represent a later transformation of isocubanite (Oudin 1983a). Several styles of exsolution of isocubanite and chalcopyrite are observed in the two chimneys. In an early stage of unmixing of Zn, Cu and Fe sulfides, chalcopyrite exsolved and formed rims around isocubanite grains, and penetrated the isocubanite as irregular lamellae (Figs. 9e,f). These assemblages are typically enclosed in wurtzite–sphalerite. In a later stage, thick chalcopyrite rims with small irregular patches of isocubanite are visible (Fig. 10a) suggesting the possibility that annealing of isocubanite led to chalcopyrite exsolution (Cabri *et al.* 1973).

Chalcopyrite is closely associated with isocubanite in the chimney interior (zone D) where it forms intergrown lamellae and patches. Euhedral crystals of chalcopyrite are also disseminated within aggregates of coarse-grained sphalerite (zone C) where they form irregular layers sub-parallel to the delicate micrometer-scale banding of colloform sphalerite (Fig. 10b).

Pyrite is a minor accessory in all zones of the chimneys, where it constitutes <1% of total sulfide content. In zones A and B, pyrite occurs as interlocking aggregates with colloform marcasite. In zone C, pyrite is more abundant and occurs both as fine-grained euhedral crystals disseminated in sphalerite grains (Fig. 7c), and within the outer rims of colloform sphalerite (Figs. 10c,d). Although usually associated with sphalerite, pyrite also occurs as free grains in siliceous gangue. Rarely, pyrite displays a finely plumose or lace-work texture around sphalerite (Figs. 10e,f).

Marcasite is relatively abundant in sample ALV-1461-4R, where it occurs mainly in zones A and D. It partly replaced euhedral pyrite crystals and displays the following textures: 1) radial growth around colloform sphalerite or around globular aggregates

MASSIVE SULFIDE SAMPLE ALV-1462-2R LONGITUDINAL CHIMNEY SECTIONS
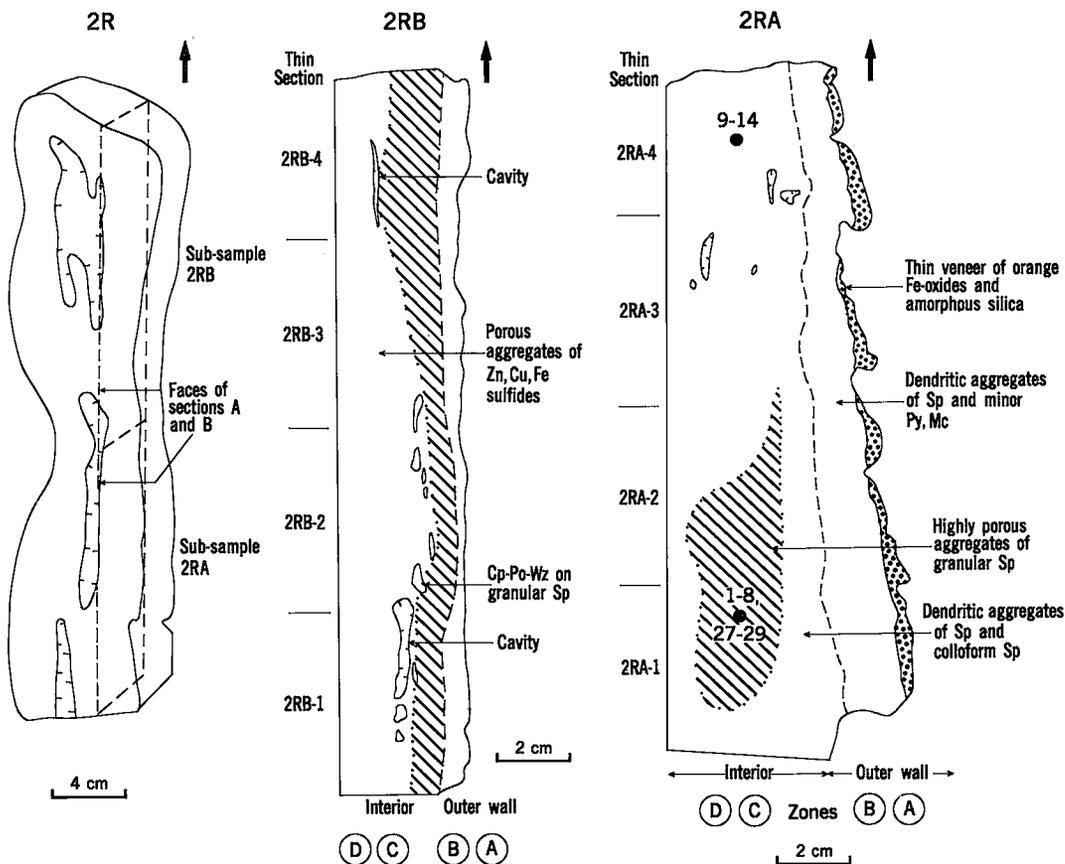
FIG. 5. Sketches of longitudinal sections of sample ALV-1462-2R. Section 2RA is lower half of chimney 2R; section 2RB is upper half. A to D correspond to zones discussed in the text. Numbered points are keyed to microprobe analyses in Tables 4 and 5. Arrow indicates top of sample. Abbreviations as in Figure 4.

of granular sphalerite crystals (Fig. 11a); 2) radiating spheroidal texture within amorphous silica (Fig. 7d); 3) interstitial overgrowth enclosing pyrite crystals (Fig. 11b); and 4) colloform texture and replacements of colloform sphalerite (Fig. 11c).

Anhydrite occurs commonly near the exterior of the chimneys as interstitial cement and infillings of cavities. It forms radiating sheaves of bladed crystals up to 1 mm long in the cavities of zone B in sample ALV-1461-4R (Figs. 7b,c). Complete or partial pseudomorphs of sphalerite and pyrrhotite after anhydrite also occur in inner zones C and D. No anhydrite was observed in sample ALV-1462-2R.

Barite forms axiolites (Fig. 11d) and porous aggregates of lath-like crystals in cavities of the outer wall (zone B) of both chimneys.

Amorphous silica occurs throughout the chimneys,

particularly in the outer zones, where it cements sulfide grains and partly fills cavities. Pseudomorphs of silica after sulfate blades and partial replacements of sulfide grains are common. Randomly oriented silica pseudomorphs after skeletal pyrrhotite have been partly replaced by sphalerite (Fig. 11e).

Other phases include unidentified Fe silicates and a kaolin–serpentine-group Fe silicate referred to here as "greenalite" (Table 10). These silicates overgrew and replaced the outer edges of iron-bearing sulfides, including pyrrhotite (Fig. 11f) and sphalerite. Microprobe analyses indicate that the greenalite-like mineral is compositionally closer to cronstedtite than greenalite which it resembles under transmitted-light microscopy. Similar "clay-like" minerals which overgrew sphalerite have been reported from 21°N EPR (Hékinian *et al.* 1980). However these phases are Si-rich and Fe-poor relative to the Plume Site silicates.

MINERALOGY: SAMPLE ALV-1462-2RB
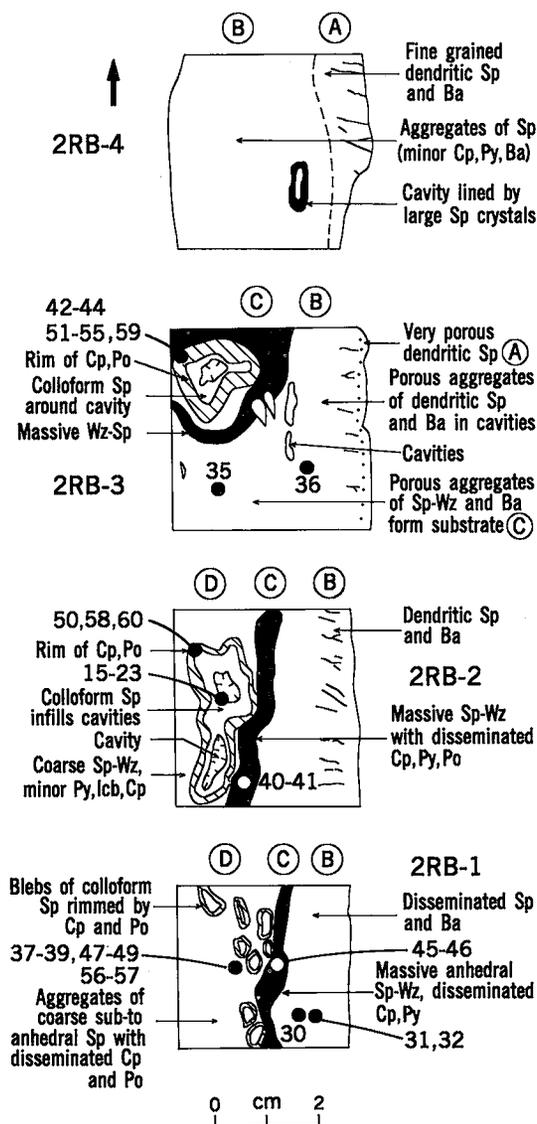
FIG. 6. Mineralogical characteristics of chimney section ALV-1462-2RB (Fig. 5). Numbered points are keyed to microprobe analyses in Tables 4 to 9. Abbreviations as in Figure 4.

PARAGENESIS OF PLUME SITE MINERALS

Sulfide and sulfate minerals in the chimneys display replacement, dissolution, and intergrowth textures. A given phase can occur both as a replacement and as a direct precipitate in the various chimney zones. In the general sequence of changes (Table 3),

the more frequent are: 1) replacement of barite and anhydrite by amorphous silica, pyrrhotite and sphalerite; 2) replacement of pyrrhotite blades by amorphous silica; 3) pseudomorphism of pyrrhotite by chalcopyrite; 4) replacement of colloform sphalerite by marcasite; and 5) transformation of isocubanite to chalcopyrite, and wurtzite to sphalerite, respectively.

The generalized paragenetic sequence of deposition of minerals is shown in Figure 12. However, the sequence must be viewed with caution because of the common dissolution and replacement of "earlier-formed" sulfides by higher temperature minerals, and because of transformations occurring in waning stages of hydrothermal activity. It is also possible that some of the "earlier-formed" minerals in the outer zones (A, B) of the chimneys formed later than interior-zone assemblages (C, D). Thus it may be more useful to consider the outer-zone assemblages as lower temperature products and the inner zone assemblages as higher temperature products. The latter are therefore more likely to have been imposed upon, or to have replaced zone (A, B) types. "Earlier-formed" textures may have formed during either waxing and waning stages of cycles of hydrothermal activity, or whenever the outer zones became thermally insulated from chimney interiors as a result of mineral precipitation in pore spaces. In our opinion, temperature is a more important parameter than time in determining the paragenetic relationships which we have observed.

CHEMISTRY OF SULFIDE MINERALS

Microprobe analyses, mainly of Zn sulfide minerals, were done to determine chemical zoning both within individual grains and along longitudinal and lateral transects across the chimneys. The results are listed in Tables 4 to 10. Each analysis number is keyed to photomicrographs in Figures 7 to 11, and sketches of the chimneys (Figs. 4–6).

Sphalerite has a wide compositional variation: Fe content ranges from 0.35 to 16.5 wt.%, although 80% of the analyses contained <7 wt.% Fe. Colloform sphalerite with fine-scale banding is Fe-poor and averages only 2.2 wt.% Fe, whereas subhedral granular sphalerite averages 4.8 wt.% Fe and wurtzite averages 12.1 wt.% Fe (Table 11). Colloform sphalerite shows oscillatory zoning; in one example, wt.% Fe changes from 4.8 to 0.35 to 1.24 between core and rim (Fig. 13c). An inverse trend from Fe-poor core of 1.13 wt.% to a slightly more enriched rim of 2.06 wt.% Fe is also observed in sample ALV-1462-2RA1 (Fig. 13a). Overall, however, colloform sphalerite varies in composition from Fe-rich cores to Fe-poor rims (Fig. 13). No systematic vertical variation in the Fe content of colloform sphalerite within the chimneys was observed. Colloform sphalerite shows color banding from almost color-
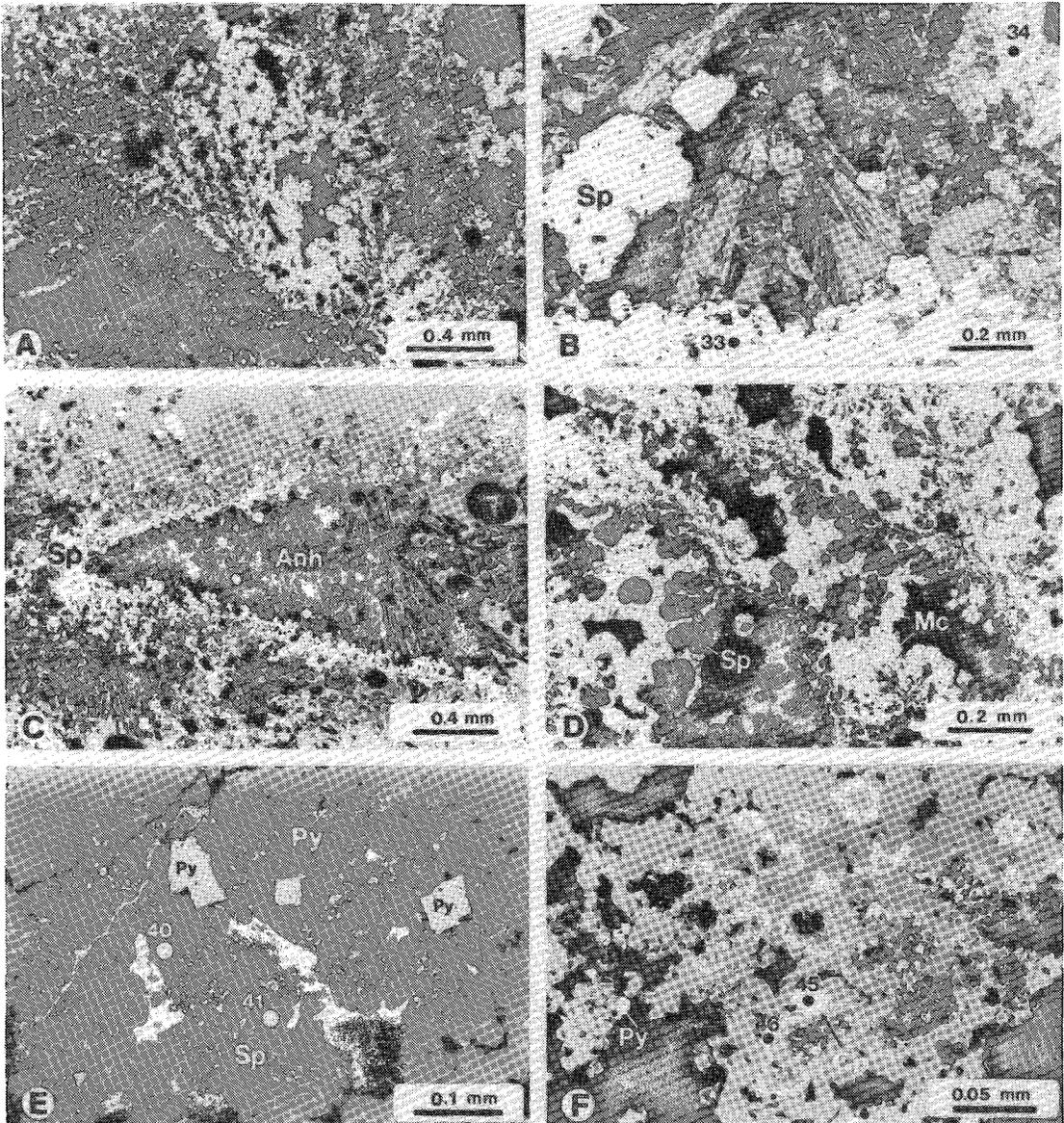
FIG. 7. (A): dendritic sphalerite. Arrow indicater points towards chimney exterior. Zone A, sample ALV-1462-2RB-1. (B): cavity filled by anhydrite crystals overgrown and surrounded by sphalerite. Zone B, sample ALV-1461-4R-3. (C): cavity filled by anhydrite crystals and surrounded by sphalerite. Zone B, sample ALV-1461-4R-3. (D): arborescent growth of colloform sphalerite enclosed in aggregate of marcasite. Zone B, sample ALV-1462-2RA-3. (E): massive aggregate of subhedral to euhedral sphalerite with disseminated fine-grained and coarse-grained euhedral pyrite. Zone C, sample ALV-1462-2RB-2. (F): nearly massive aggregate of sphalerite with colloform chalcopyrite overgrowths. Zone C, sample ALV-1462-2RB-1.

less Fe-poor rims to opaque Fe-rich cores. In other cases, the microscale banding is due to fine silica impregnations and interlayers, and the presence of more porous sphalerite bands. Most of the analyses of colloform sphalerite have low totals due to the presence of dispersed silica (detected on the EDS). Oscillatory zoning may be due to variations both in Fe and Si contents.

TABLE 1. CHARACTERISTICS OF MINERALS FROM TWO Zn-RICH CHIMNEYS FROM SOUTHERN JUAN DE FUCA RIDGE

Mineral	Occurrence
Sphalerite (Zn, Fe) S	– Irregular anhedral masses with disseminated grains of Cp, Po, Py, Mc. – Aggregates of fine-grained dendrites. – Colloform globules and aggregates of colloform growth forms with delicate micrometer-scale layering. – Aggregates of coarse-grained subhedral to euhedral grains.
Pyrite FeS_2	– Fine-grained disseminated subhedral to euhedral crystals in Sp. – Single euhedral grains occurring at the outer edge of Sp crystals; clusters of crystals that form thin layers at the outer edge of colloform Sp. – Cubes disseminated in gangue (closely associated with Sp). – Anhedral to euhedral crystals intergrown with Mc. – Very fine-grained dendritic textures (rare).
Marcasite FeS_2	– Aggregates of subhedral to euhedral crystals disseminated in gangue but closely associated with Sp. – Radiating colloform textures and spheroidal textures in gangue or bordering colloform Sp. – Subhedral intergrowths with pyrite, forming massive aggregates.
Pyrrhotite $Fe_{(1-x)}S$	– Tabular crystals (<0.1 mm long) distributed around colloform Sp and closely associated with chalcopyrite.
Chalcopyrite $CuFeS_2$	– Euhedral crystals associated with Sp and Icb.
Wurtzite (Zn, Fe) S	– Euhedral hexagonal crystals (iron-rich).
Isocubanite $CuFe_2S_3$	– Euhedral crystals associated with Cp.
Barite $BaSO_4$	– Small laths (0.1 mm long) as radial clusters in cavities.
Anhydrite $CaSO_4$	– Sheaves and clusters of acicular crystals. – Radiating aggregates of relatively large crystals (<1 mm long) in cavities.
Amorphous Silica	– Veneer of amorphous white silica on outer wall of chimney. – Porous siliceous matrix enclosing and replacing sulfides.
"Greenalite"	– Bluish kaolin serpentine-group mineral that overgrew and replaced Sp, Po and an iron silicate mineral.

Abbreviations: Sp sphalerite, Wz wurtzite, Cp Chalcopyrite, Icb isocubanite, Py pyrite, Po pyrrhotite, Mc marcasite.

TABLE 2. VISUAL ESTIMATE OF MINERAL ABUNDANCES IN SAMPLES ALV-1461-4R AND ALV-1462-2R (VOL.%)

SAMPLE	Sp	Py	Po	Cp	Mc	Gre	TOTAL	Silica Gangue	POROSITY
4R-1	50	<1	10	<2	<5	<0.5	65	10-15	20-25
4R-2	50-55	1	<5	1	<10	<0.5	70	5-6	20-25
4R-3	50-55	2	<3	<1	5	<0.5	65	5-6	30
4R-4	55	<1	2	1	2-3	<0.5	60	10	30
2RB-1	85	1	2-3	1-2		<0.5	90	5	5
2RB-2	70-75	1	10	5		<0.5	85-90	<5	5-10
2RB-3	70-75	1	<10	<5		<0.5	85	5-10	5-10
2RB-4	75-80	1	<0.5	<0.5		<0.5	80	15	5
2RA-1	90	<1	<0.5	<0.5		<0.5	90	1	5
2RA-2	95	1	tr	<0.5		<0.5	95	<1	5
2RA-3	70	1	tr	<1	10	<0.5	80	<1	20
2RA-4	50	1	tr	<0.5	25	<0.5	75	<1	25

Abbreviations: Sp sphalerite, Py pyrite, Po pyrrhotite, Cp chalcopyrite, Mc marcasite, Gre "greenalite".

Lateral variations in the Fe content of sphalerite follow the textural variations of sphalerite observed across the zones of the chimneys, e.g., Fe-rich granular sphalerite–wurtzite and Fe-poor dendritic sphalerite dominate the inner zones and outer zones, respectively. Fe content in wurtzite decreases toward the center of the chimneys. Variation in the Fe content of granular sphalerite and wurtzite within chimney ALV-1462-2R is shown in Figure 14. A broad increase in iron content is observed from the lower

part to the upper part of the interior of the chimney.

Colloform and granular sphalerite contain 0 to 0.56 wt.% Cd (average 0.2 wt.%); Cd and Fe show a broad positive correlation ($r = 0.62$) for colloform sphalerite and an excellent positive correlation ($r = 0.89$) for the granular sphalerite. Wurtzite contains 0.04 to 0.71 wt.% Cd (average 0.3 wt.%) and correlation between Cd and Fe is poor ($r = 0.53$). Variations in Fe and Cd contents of Zn sulfides probably reflect changes in fluid chemistry (i.e., trace-metal levels or S fugacity) or temperature, or both (Koski et al. 1984). Chalcopyrite contains detectable amounts of Zn, Cd, Mn and Ag. The maximum Zn content in chalcopyrite is 1.04 wt.% and the average is 0.46 wt.% (Table 11). Isocubanite has average Fe and Zn contents of 42 and 0.5 wt.%, respectively.

The compositions of these mineral phases from the Plume Site closely resemble those from the same area described by Koski et al. (1984). The compositions are also similar to those from the EPR at 21°N (Styrt et al. 1981).

DISCUSSION

Relations between fluid chemistry and mineralogy

The chimneys at Plume Site are exceptionally Zn-rich compared to Fe, Cu, Zn samples from 13°N
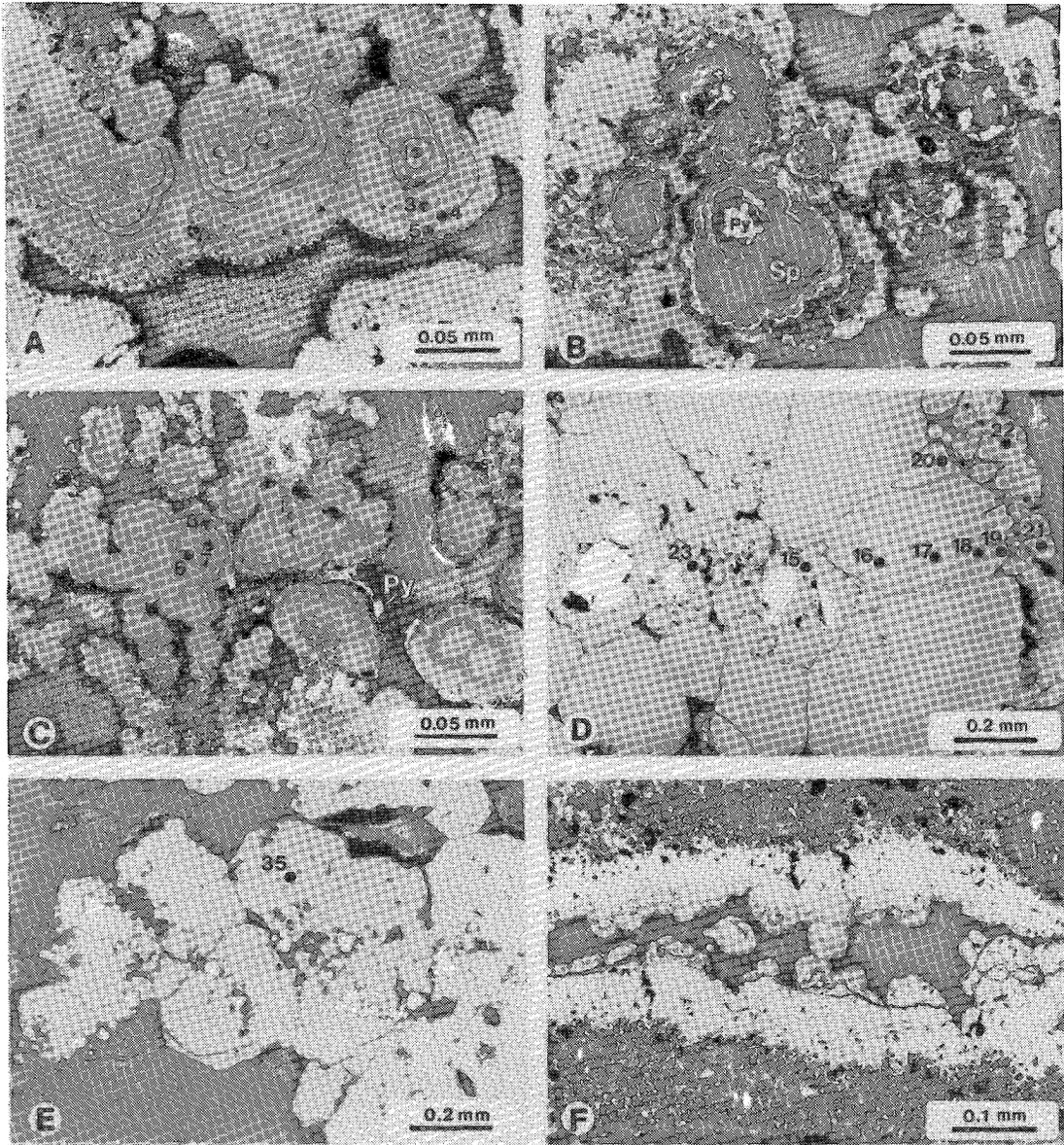
FIG. 8. (A): coalesced globules of colloform sphalerite with delicate growth banding. Zone D, sample ALV-1462-2RA-1. (B): colloform sphalerite with well-defined μm-scale banding. Late pyrite occurs in centers and rims of some sphalerite grains. Zone D, sample ALV-1462-2RA-2. (C): globular colloform sphalerite with μm-scale banding and overgrowths of pyrite. Zone D, sample ALV-1462-2RA-1. (D): broadly zoned colloform sphalerite around euhedral chalcopyrite. Zone D, sample ALV-1462-2RB-2. (E): coarse grains of ZnS with hexagonal outline (possibly wurtzite). White crystals are pyrite. Zone D, sample ALV-1462-2RB-3. (F): elongate cavity lined by colloform sphalerite. Zone D, sample ALV-1462-2RA-4.

and 21°N EPR described by Hékinian *et al.* (1984), Lafitte *et al.* (1984, 1985), Zierenberg *et al.* (1984), Goldfarb *et al.* (1983), and Oudin (1983a), and to the Fe-, Cu-rich, and Zn-poor samples from the Galapagos Rift (Malahoff 1982, Embley *et al.* 1988).

However, they are comparable to those sampled at Axial Seamount (Hannington & Scott 1988) and upper zones of the Parizeau deposit, Explorer Ridge (Hannington *et al.* 1985, quoted by Gross & McLeod 1988).
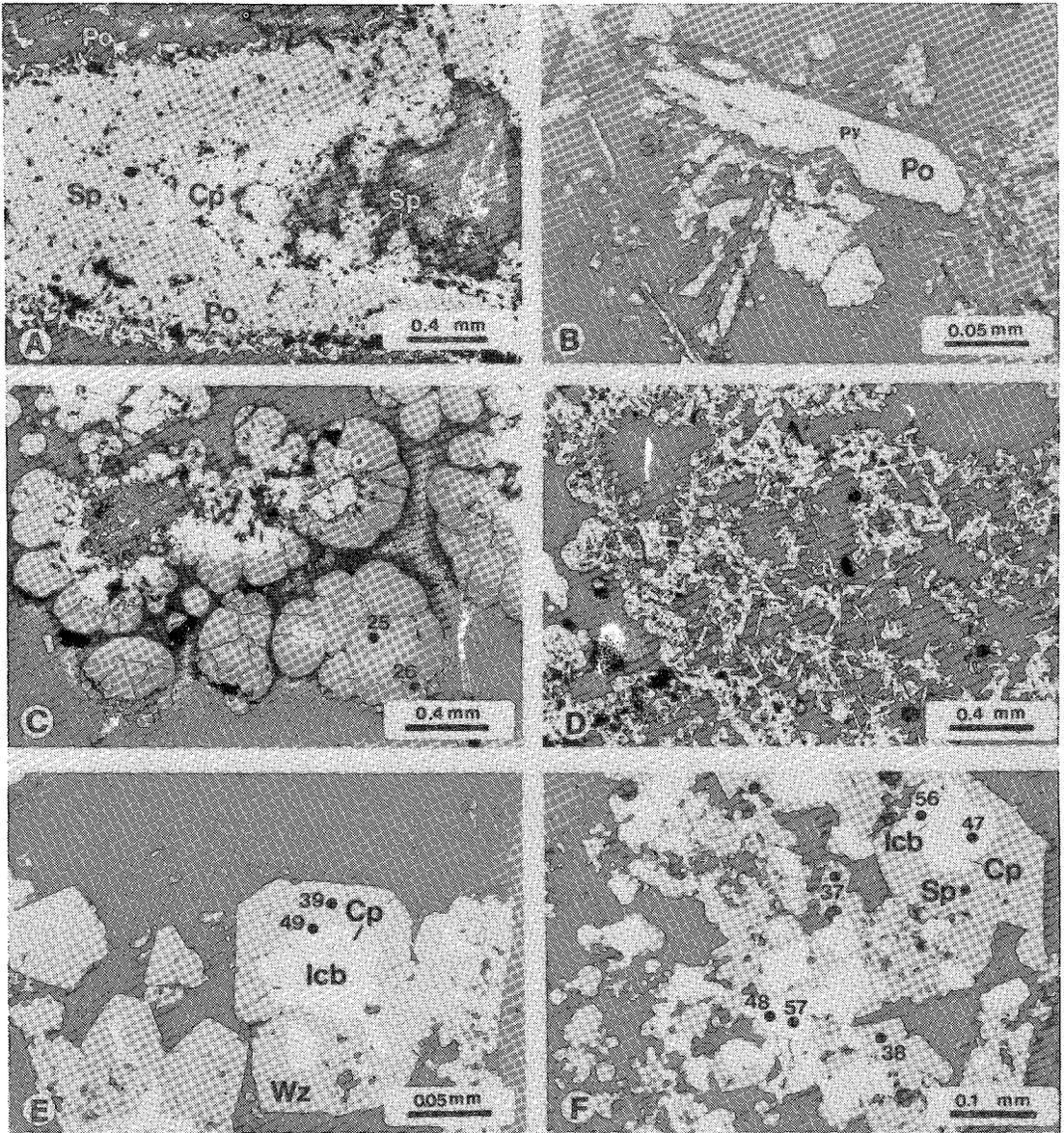
Fig. 9. (A): part of an elongate cavity lined by sphalerite, chalcopyrite, and pyrrhotite. Zone D, Sample ALV-1461-4R-1. (B): primary pyrrhotite crystals partly replaced by silica. Pyrrhotite also contains small pyrite blebs. Zone D, sample ALV-1461-4R-1. (C): pyrrhotite and chalcopyrite partly filled a cavity within colloform sphalerite. Zone D, sample ALV-1461-4R-3. (D): randomly oriented pyrrhotite blades associated with sphalerite. Zone D, sample ALV-1461-4R-1. (E): wurtzite around isocubanite core which has a thin rim of chalcopyrite. Zone D, sample ALV-1462-2RB-1. (F): subhedral sphalerite around chalcopyrite with isocubanite core. Zone D, sample ALV-1462-2RB-1.

Vent fluids from southern Juan de Fuca Ridge are highly enriched in Fe, Zn, Ba, Mn, Cl, Ca, Sr and K compared to seawater. They are also enriched when compared to fluids from 21°N, 13°N, and Galapagos Rift. They are compositionally similar to 13°N but of much higher concentrations. For example, Fe is about 10 times higher, Zn is 9 times higher, Mn is 4 times higher, and Cl is 1.5 times higher. By contrast, H_2S and Cu levels are depleted, and SiO_2 and pH values are comparable (Von Damm &
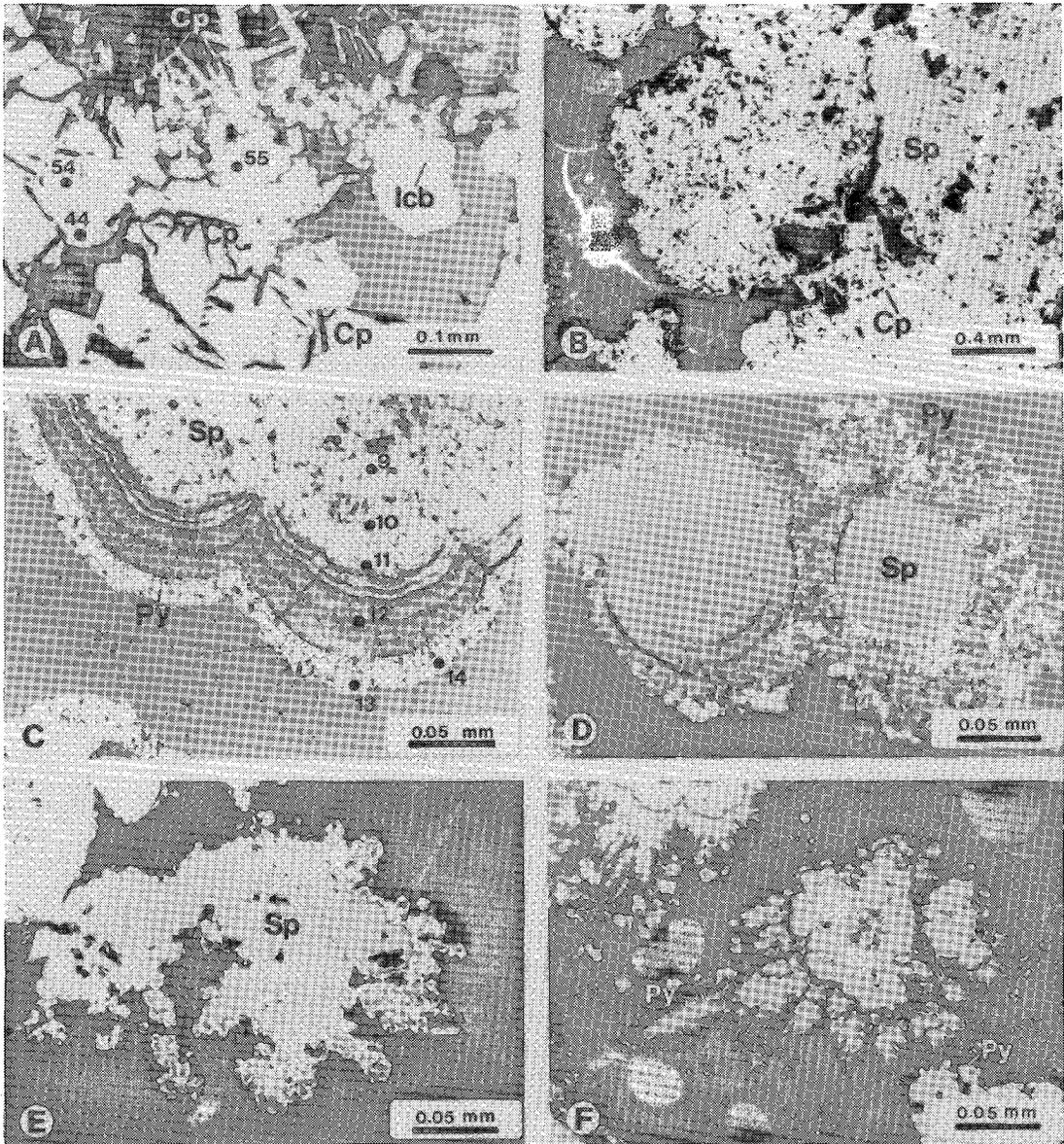
FIG. 10. (A): euhedral to subhedral chalcopyrite intergrown with isocubanite. Exsolved chalcopyrite blades are visible near top. Zone D, sample ALV-1462-2RB-3. (B): aggregate of subhedral sphalerite with several μm-scale bands of chalcopyrite. Zone C, sample ALV-1461-4R-4. (C): colloform sphalerite with well-defined μm-scale banding and rim of euhedral pyrite. Zone C, sample ALV-1462-2RA-4. (D): spheroidal sphalerite with some fine-scale banding. Small pyrite and sphalerite crystals surround the spheroids. Zone C, sample ALV-1462-2RA-1. (E): fine-grained pyrite as a lace-work around anhedral sphalerite. Zone C, sample ALV-1461-4R-3. (F): fine-grained plumose pyrite that replaced sphalerite. Zone C, ALV-1462-2RA-3.

Bischoff 1987, Philpotts *et al.* 1987). Two of the vent fluids studied are from Plume Site and were collected within 10 m of chimney ALV-1462-2R (Fig. 3). The high Zn and Fe, and low Cu contents of these fluids are consistent with the observed sulfide mineralogy described for Plume Site (USGS Juan de Fuca Study Group 1986). According to thermodynamic calculations, the fluids are supersaturated at natural pH
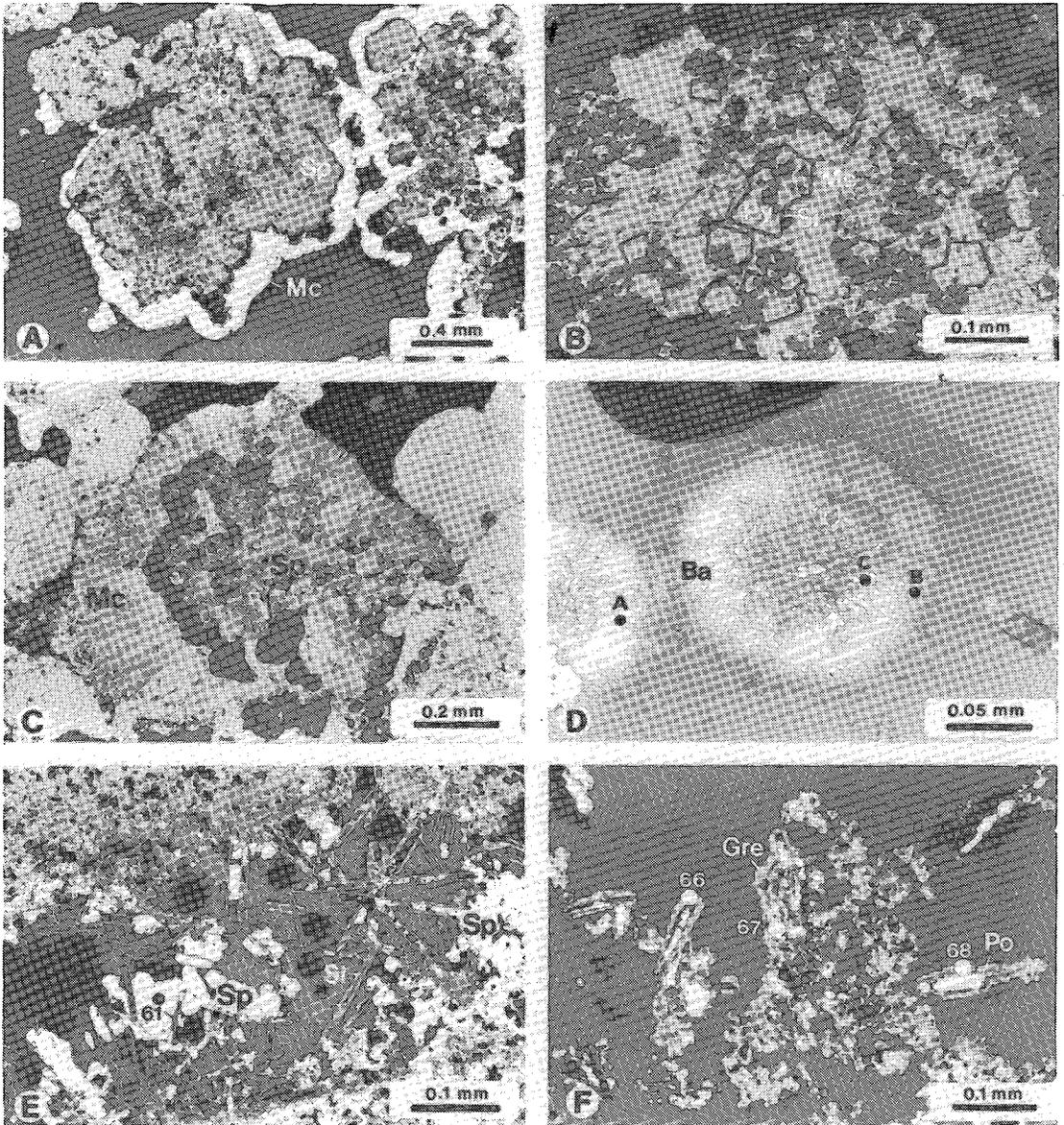
FIG. 11. (A): sphalerite surrounded by rim of radiating marcasite. Zone D, sample ALV-1461-4R-1. (B): euhedral pyrite crystals overgrown by silica are surrounded by marcasite crystals. Zone B, sample ALV-1462-2RA-1. (C): globular colloform sphalerite enclosed in radiating marcasite. Zone B, sample ALV-1462-2RA-3. (D): radiating clusters of barite. Microprobe analyses indicate barite with minor Sr and Ca at points A and B, and sphalerite with traces of Ba at point C. Zone B, sample ALV-1461-4R-3. (E): randomly oriented blades of amorphous silica after pyrrhotite. Centers of blades are partly replaced by sphalerite. Zone B, sample ALV-1462-2RB-1. (F): primary pyrrhotite crystals partly replaced by silica, and surrounded by "Greenalite" (possibly cronstedtite). Zone D, sample ALV-1461-4R-2.

(3.3) in sphalerite, wurtzite, pyrrhotite, silica, barite, pyrite, gypsum, and aluminosilicates (Philpotts *et al.* 1987). These are the important constituents of the Plume Site chimneys. Philpotts *et al.* (1987) specu-

lated that the extent of silicate supersaturation indicates buffering of high-temperature fluids by basalt–greenstone silicates. Von Damm & Bischoff (1987) interpreted the vent fluid compositions as the result

of interaction of high-temperature fluids and cold seawater in the subsurface, leading to precipitation of metal sulfides and sulfates and low exit temperatures.

The maximum exit temperature measured was 285°C at Vent 1, and 224°C at Plume Site (USGS Juan de Fuca Study Group 1986). Preliminary fluid-inclusion data on wurtzite crystals indicated filling temperatures of between 150 and 250°C (Koski *et al.* 1984). One measurement on an anhydrite crystal from Vent 1 yielded a temperature of 285°C (Brett *et al.* 1987). These temperatures are similar to the $\geq 340°C$ (based on quartz geobarometry-geothermometry) for fluid temperatures at depth, prior to mixing with cold seawater (Von Damm & Bischoff 1987).

An upper limit of 328°C was inferred for the mineral assemblage isocubanite + pyrrhotite + chalcopyrite for an interior conduit in a chimney sample from Vent 1 (Brett *et al.* 1987) based on experimental work by Yund & Kellerud (1966). Compositions of wurtzite, chalcopyrite, and pyrrhotite from interior conduits in chimney ALV-1462-2R (Tables 6, 7, 9 and 11) agree very closely with those determined experimentally at 300°C for the system chalcopyrite + pyrrhotite + sphalerite + pyrite. Moreover, there is also good agreement between the composition of isocubanite from Plume Site chimneys (Tables 8, 11) and the composition determined at 300°C for the system isocubanite + pyrrhotite + sphalerite (Kojima & Sugaki 1985). Therefore, the best estimate for the temperature of formation of the high-temperature assemblages at Plume Site is about 300°C.

Little can be deduced from the present study on the effects of source-rock composition on the fluid chemistry and chimney mineralogy of southern Juan de Fuca Ridge. There is general agreement that compositions of fresh ocean-floor basalts are likely very similar here and elsewhere along the East Pacific ridge crests (Philpotts *et al.* 1987, Von Damm & Bischoff 1987, Hannington & Scott 1988). Other factors, such as differences in alteration styles and subsurface processes involving mixing of fluids and generation of new mineral assemblages, are thought to be more important.

The relative ages and maturities of different hydrothermal systems and deposits may influence chimney mineralogy. Small, young, immature systems such as southern Juan de Fuca Ridge (Koski *et al.* 1984) and Axial Seamount (Hannington & Scott 1988, Jonasson *et al.* unpub.) are Zn-, Fe-rich and Cu-poor, whereas older, more mature systems such as Galapagos Rift (85°50') and 21°N tend to be much richer in Fe and Cu, and poorer in Zn (Embley *et al.* 1988, Lafitte *et al.* 1985). However, such generalizations are suspect given that more young chimney material than older, reworked mound material is commonly sampled on submersible-based expedi-

TABLE 3. SEQUENCE OF TRANSFORMATION AMONGST PLUME SITE MINERALS

Original mineral	1st transformation	2nd transformation	3rd transformation
ANHYDRITE	dissolution	amorphous silica	pyrrhotite
BARITE	dissolution	amorphous silica	sphalerite
ALL SULFIDES	amorphous silica		
PYRRHOTITE	i) dissolution	amorphous silica	sphalerite
	ii) dissolution	sphalerite	"greenalite"
	iii) chalcopyrite		
	iv) pyrite		
ISOCUBANITE	chalcopyrite		
PYRITE	chalcopyrite		
MARCASITE	pyrite		
SPHALERITE	i) marcasite		
	ii) chalcopyrite		
	iii) "greenalite"		
WURTZITE	sphalerite		
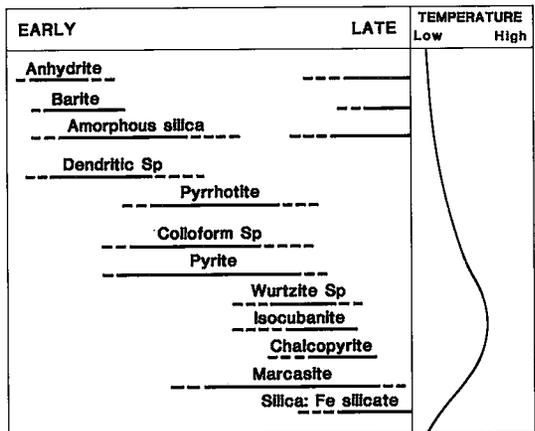
FIG. 12. Generalized paragenetic relationships of minerals from the Plume Site.

TABLE 4. MICROPROBE ANALYSES OF COLLOFORM SPHALERITE FROM CHIMNEYS ALV-1462-2R and ALV-1462-4R.

#	Section	Zone	Fig.	Cu	Fe	Zn	Cd	Ag	S	TOTAL
1	2RA-1	D	8a	0.00	1.13	62.97	0.03	0.04	32.09	96.27
2	2RA-1	D	8a	0.06	1.25	64.48	0.18	0.00	32.78	98.80
3	2RA-1	D	8a	0.08	1.31	63.21	0.16	0.04	32.78	97.60
4	2RA-1	D	8a	0.01	1.44	61.28	0.00	0.06	31.18	93.99
5	2RA-1	D	8a	0.01	2.06	62.69	0.00	0.07	32.05	96.90
6	2RA-1	D	8c	0.03	1.12	63.53	0.07	0.06	32.48	97.32
7	2RA-1	D	8c	0.04	1.04	63.48	0.15	0.02	32.51	97.24
8	2RA-1	D	8c	0.04	0.99	63.46	0.11	0.04	32.94	97.59
9	2RA-4	C	10c	0.19	6.50	58.44	0.33	0.12	33.13	98.71
10	2RA-4	C	10c	0.48	6.53	57.80	0.45	0.20	32.89	98.38
11	2RA-4	C	10c	0.55	2.25	61.03	0.47	0.15	32.59	98.05
12	2RA-4	C	10c	0.07	1.26	58.20	0.15	0.01	30.17	89.86
13	2RA-4	C	10c	0.02	2.47	63.31	0.06	0.00	33.30	99.19
14	2RA-4	C	10c	0.01	2.73	62.99	0.04	0.06	33.09	98.93
15	2RB-2	D	8d	0.18	3.79	61.56	0.36	0.02	33.18	99.11
16	2RB-2	D	8d	0.51	3.30	62.02	0.56	0.21	32.93	99.54
17	2RB-2	D	8d	0.03	0.35	62.94	0.23	0.00	32.69	96.25
18	2RB-2	D	8d	0.03	0.48	60.81	0.06	0.00	32.39	93.77
19	2RB-2	D	8d	0.02	0.79	60.56	0.07	0.00	32.75	94.18
20	2RB-2	D	8d	0.02	0.54	61.18	0.01	0.00	32.82	94.59
21	2RB-2	D	8d	0.02	1.30	59.21	0.05	0.00	31.51	92.12
22	2RB-2	D	8d	0.04	1.24	59.41	0.09	0.00	37.71	92.59
23	2RB-2	D	8d	0.37	4.80	59.83	0.37	0.00	33.47	98.94
24	4R-2	D		0.47	11.70	53.94	0.41	0.04	34.30	100.89
25	4R-3	D	9c	0.01	2.80	62.41	0.06	0.00	33.31	98.59
26	4R-3	D	9c	0.00	2.73	61.64	0.04	0.00	32.84	97.27

Mn < 0.05 wt.%

TABLE 5. MICROPROBE ANALYSES OF GRANULAR SPHALERITES FROM CHIMNEYS
ALV-1462-2R and ALV-1461-4R.

#	Section	Zone	Fig.	Cu	Fe	Zn	Cd	Ag	S	TOTAL
27	2RA-1	D		0.05	6.61	56.76	0.19	0.02	32.67	96.30
28	2RA-1	D		0.03	2.83	53.66	0.09	0.00	28.68	85.31
29	2RA-1	D		0.00	3.62	61.99	0.08	0.00	33.36	99.08
30	2RB-1	B		0.09	5.13	56.33	0.10	0.10	31.33	93.08
31	2RB-1	B		0.13	6.99	58.41	0.44	0.00	33.22	99.19
32	2RB-1	B		0.15	9.77	55.08	0.39	0.01	33.50	98.91
33	4R-3	B	7b	0.00	0.81	63.56	0.00	0.02	32.74	97.14
34	4R-3	B	7b	0.01	0.87	63.98	0.00	0.00	32.77	97.65

Mn < 0.02 wt.%

TABLE 6. MICROPROBE ANALYSES OF WURTZITE FROM CHIMNEY ALV-1462-2R.

#	Section	Zone	Fig.	Cu	Fe	Zn	Cd	Ag	S	TOTAL
35	2RB-3	C	8e	0.81	6.52	57.97	0.18	0.08	32.96	98.54
36	2RB-3	B		0.22	16.55	48.45	0.35	0.02	33.88	99.50
37	2RB-1	D	9f	0.48	8.00	57.51	0.04	0.01	33.40	99.45
38	2RB-1	D	9f	0.27	14.27	50.26	0.08	0.00	33.88	98.77
39	2RB-1	D	9e	0.32	13.07	51.18	0.50	0.09	33.78	98.95
40	2RB-2	C	7e	0.34	11.16	53.83	0.28	0.05	33.77	99.44
41	2RB-2	C	7e	0.15	14.84	49.62	0.71	0.07	33.93	99.33

Mn < 0.03 wt.%

TABLE 7. MICROPROBE ANALYSES OF CHALCOPYRITE FROM CHIMNEY ALV-1462-2R.

#	Section	Zone	Fig.	Cu	Fe	Zn	Cd	Ag	S	TOTAL
42	2RB-3	D		32.55	32.15	0.28	0.03	0.06	34.81	99.89
43	2RB-3	D		32.40	32.60	0.17	0.07	0.06	35.25	100.59
44	2RB-3	D	10a	32.15	32.30	0.36	0.01	0.05	34.78	99.65
45	2RB-1	C	7f	32.13	31.43	1.04	0.03	0.01	34.69	99.33
46	2RB-1	C	7f	32.12	31.49	0.81	0.01	0.01	34.39	98.83
47	2RB-1	D	9e	31.95	32.54	0.29	0.05	0.15	34.77	99.76
48	2RB-1	D	9f	31.71	32.64	0.26	0.05	0.04	34.84	99.54
49	2RB-1	D	9e	32.49	31.64	0.72	0.02	0.07	34.86	99.80
50	2RB-2	D		32.22	32.34	0.22	0.04	0.06	35.46	100.36

Mn < 0.05 wt.%

TABLE 8. MICROPROBE ANALYSES OF ISOCUBANITE FROM CHIMNEY ALV-1462-2R.

#	Section	Zone	Fig.	Cu	Fe	Zn	Cd	Ag	S	TOTAL
51	2RB-3	D		21.47	42.21	0.44	0.02	0.08	35.24	99.47
52	2RB-3	D		21.29	42.75	0.46	0.01	0.05	35.37	99.95
53	2RB-3	D		21.54	42.44	0.38	0.02	0.05	35.40	99.92
54	2RB-3	D	10a	21.03	42.01	0.39	0.03	0.08	35.14	98.71
55	2RB-3	D	10a	20.88	42.44	0.39	0.01	0.04	35.18	98.95
56	2RB-1	D	9f	22.09	40.99	0.55	0.02	0.07	35.40	99.12
57	2RB-1	D	9f	21.56	41.26	0.71	0.01	0.06	35.05	98.65
58	2RB-2	D		21.13	42.10	0.50	0.07	0.09	35.94	99.83

Mn < 0.07 wt.%

TABLE 9. MICROPROBE ANALYSES OF PYRRHOTITE FROM CHIMNEYS ALV-1462-2R
AND ALV-1461-4R.

#	Section	Zone	Fig.	Cu	Fe	Zn	Cd	Ag	S	TOTAL
59	2RB-3	D		0.06	60.05	0.02	0.04	0.07	39.38	99.62
60	2RB-2	D		0.01	60.13	0.04	0.00	0.05	39.55	99.80
61	2RB-1	B	11e	0.04	59.37	0.07	0.00	0.04	39.26	98.78
62	4R-2	D		0.03	59.54	0.00	0.02	0.04	39.78	99.42

Mn <0.02 wt.%

TABLE 10. MICROPROBE ANALYSES (WT.%) OF "GREENALITE"
FROM CHIMNEY ALV-1461-4R.

	4R-2 #66	4R-2 #67	4R-2 #68
SiO2	18.04	18.04	18.75
Al2O3	0.02	0.02	0.04
TiO2	-	-	-
FeO	68.20	68.93	68.75
MgO	1.83	1.35	1.42
Na2O	-	-	-
CaO	-	-	-
K2O	-	-	-
MnO	0.51	0.36	0.30
TOTAL	88.60	88.70	89.26

"greenalite" formula:
$(Fe^{+2}_{1.96} Mg_{0.04})(Fe^{+3})(Fe^{+3}_{0.05} Si_{0.95})O_5(OH)_4$

TABLE 11. AVERAGE WT% CONTENT BY ELEMENT OF SULFIDE
MINERALS FROM THE PLUME SITE.

	Coll. Sp N=24*		Gran. Sp N=7*		Wz N=7		Cp N=9		Icb N=8		Po N=4	
	$\bar{x}$	σ	$\bar{x}$	σ	$\bar{x}$	σ	$\bar{x}$	σ	$\bar{x}$	σ	$\bar{x}$	σ
Fe	2.2	1.7	4.8	3.0	12.1	3.4	32.1	0.5	42.0	0.6	59.7	0.3
Cd	0.2	0.2	0.2	0.2	0.3	0.2	-		-		-	
Cu	0.2	0.1	0.1	0.01	0.4	0.2	32.2	0.3	21.4	0.4	0.1	0.02
Zn	61.7	1.7	59.4	3.4	52.7	3.5	0.5	0.3	0.5	0.1	0.1	0.03
S	32.9	1.1	32.8	0.7	33.6	0.3	34.9	0.3	35.4	0.3	39.5	2.0

Abbreviations: Sp sphalerite, Wz wurtzite, Cp chalcopyrite, Po pyrrhotite,
Icb isocubanite, Gran. Granular, Coll. Colloform, N Number of analyses.
* Analyses 12 and 28 are not included in the calculations because of their
low totals wt.%.

tions. The nature of metal sulfide zoning and effects of later zone-refining are generally unknown in most seafloor deposits.

Mineral chemistry

Interpretations of much of the mineral chemistry in the Plume Site chimneys are in close agreement with those of Koski *et al.* (1984) and will be summarized briefly here. However, some differences were noted. Marcasite commonly replaced the walls of worm tubes or the remains of other organisms and formed crusts on the outer walls of chimneys. It may form by several mechanisms involving the direct precipitation of Fe sulfide as hydrothermal fluids percolate through chimney walls to the outer shell, by reaction of hydrothermal Fe with S associated with decaying organisms, or by direct precipitation within organic substrates. According to Murowchick & Barnes (1986), marcasite precipitates at pH ≤ 5 (25°C) by direct reaction of Fe with H_2S and oxidative polysulfide (S_n^{2-}) derivatives. Direct reaction with polysulfide ions favors precipitation of marcasite over pyrite. In this case, restricted oxidation of hydrogen sulfide can result from simple mixing of oxic seawater (pH 8.2) with hydrothermal fluid (pH 3.3) in pore spaces. However, the close spatial associ-

ation with organic remains is not explained. Juniper *et al.* (1986) measured high percentage levels of both Fe and elemental S (plus some organic sulfur) in mucus exudates on polychaete worms (Axial Seamount, Explorer Ridge). Marcasite can form directly from such a mixture as the organic matter degrades. Clearly, interaction of Fe from cool hydrothermal fluid with mucus would precipitate marcasite at pH ≤5 and pyrite at higher pH. Tunnicliffe & Fontaine (1987) demonstrated that ZnS minerals can form under similar circumstances in worm mucus on chimneys at southern Juan de Fuca Ridge. Unless worm communities were suddenly overwhelmed by burgeoning chimney growth, these mineral syntheses would be low-temperature processes.

The distribution of Fe in sphalerite (and wurtzite) is exactly as found by Koski *et al.* (1984). In all cases it can be argued that Fe (and perhaps Cd) levels are functions of changes in temperature and sulfur fugacity of hydrothermal fluid (Scott & Kissin 1973). For example, the increase in Fe content in colloform sphalerite from core to rim could be due to increasing temperature, decreasing sulfur fugacity, or both. Similarly, lateral variation of iron content (increasing inward) of Zn sulfides is probably a function of increasing temperature; morphological changes and a phase change from sphalerite to wurtzite from zones A to D are consistent with this interpretation (Scott & Barnes 1972). Increase in Fe content of Zn sulfides vertically upwards may depend on the relative importance of a number of factors. Chimney ALV-1462-2R is richer in granular sphalerite in its lower half and in wurtzite–sphalerite in its top half. Since chimneys grow upwards as well as outwards, the change in Fe content and polymorph proportions may be accounted for by a temperature increase or a decline in sulfur fugacity. The latter may reflect changes in fluid chemistry at depth, or result from rapid sulfide precipitation promoted by mixing with seawater, or oxidation of H_2S. However, these processes would likely be accompanied by a significant decrease in temperature. Given that there is no other indication of mineralogical change over the vertical section, an intensifying hydrothermal system rather than a declining one is favored to explain the Fe zonation in Zn sulfides.

Changes from strong positive correlations between Fe and Cd in granular sphalerite ($r = 0.89$) to poor correlations in wurtzite ($r = 0.53$) are not readily explained but do indicate that granular sphalerite probably did not form from wurtzite inversion (a low-temperature transformation).

Models for chimney growth

The composition and textural characteristics of the two chimneys described in the previous sections are used to develop a plausible model of chimney growth. Initial growth of the chimneys (zones A, B)
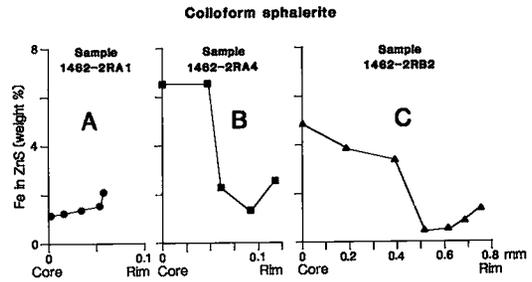
FIG. 13. Variations of wt.% Fe from the cores (at zero mm) to the rims of colloform sphalerite (three separate traverses are shown) in three samples from chimney ALV-1462-2R.
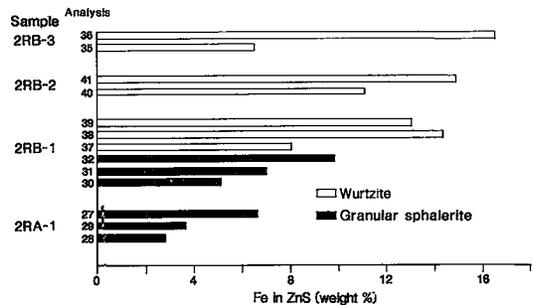
FIG. 14. Variations of wt.% Fe in granular sphalerite and wurtzite from sample ALV-1462-2R. Microprobe analyses are listed in Tables 5 and 6.

seems to have taken place through primary quench deposition of outward-growing dendrites of fine-grained sphalerite with minor pyrite and marcasite. Two different processes seem to have been operative; much of the dendritic sphalerite grew into open spaces (ALV-1462-2R) and formed its own scaffolding, but some may have precipitated interstitially within a shell composed of anhydrite blades and amorphous silica. One of the authors (I.R.J.) has observed a growth of a bladed anhydrite mass 10–15 cm thick over a two-day period at a high-temperature vent (330°C) on Axial Seamount. A sample was found to be impregnated by tiny black sphalerite crystals aligned along the faces of interlocking anhydrite blades. The initial rapid-quench stage was followed by thickening of the primitive shell through local precipitation of fine-grained colloform sphalerite, outward-growing dendritic sphalerite, and amorphous silica. This second sequence of early events also seems to have occurred at the Plume Site (ALV-1461-4R). Such precipitates served to reduce porosity, increasingly insulated the interior conduit from inwardly-drawn cold seawater, and inhibited mixing of fluids. Low-temperature

deposition of pyrite and marcasite took place in the outer zones, and early-formed anhydrite redissolved.

The next stages in development of chimneys at Plume Site resulted from thermal insulation and increased temperatures of the venting fluids, that lead to inward-growing precipitation of the higher temperature assemblages: Fe-rich granular sphalerite and chalcopyrite (zone C), and wurtzite and Cu and Fe sulfides within interior conduits (zone D).

Pyrrhotite is largely restricted to these interior zones C and D, and appears to be earlier than some coarse-grained colloform sphalerite. Chalcopyrite also occurs in zones C and D, in association with rare isocubanite and Fe sulfides. Pyrite and marcasite were precipitated throughout most of the interval of Zn-sulfide deposition mainly in the outer zones of the chimneys; late marcasite replaced and overgrew colloform sphalerite and developed as crusts within worm remains on the outer wall surfaces.

Mineralogical zonations and changes occurring in the two chimneys (Table 3) are a consequence of fluctuations in fluid chemistry as well as in the environment of deposition (e.g., temperature, porosity, and permeability of chimney matter) as discussed previously. These transformations result from interaction of upwelling hot hydrothermal fluids and cold ocean water drawn through the porous wall (Haymon & Kastner 1981, Oudin 1983b, Tivey & Delaney 1986). The nature of this process has been well-demonstrated by Shanks & Seyfried (1987) who examined a cross-section of ALV-1461-4R for S isotope zonation. Isotopically lighter S is found near the interior conduits. The outer zones of ^{34}S enrichment reflect mixing of S derived from in-drawn seawater sulfate and mantle-derived H_2S. Sulfate must undergo reduction within the chimney pore spaces by reaction with Fe(II) for this zonation to be established.

Low-temperature hydrothermal changes observed in the Plume Site chimneys include alteration of Cu, Zn, and Fe sulfides to oxides in the outer walls, inversion of wurtzite to sphalerite, and late replacement of sulfides by silica and Fe silicates (Table 3). The last process suggests that the fluids were depleted in sulfur, but were charged with sufficient silica to inhibit iron hydrolysis and iron oxide formation. All of these transformations are characteristic of the waning stages of hydrothermal activity (Laffite et al. 1985, Koski et al. 1984, Zierenberg et al. 1984, Goldfarb et al. 1983, Oudin 1983a, Oudin et al. 1981).

CONCLUSIONS

All of the mineralogical zonations, chemistry, and mineral changes described above are in full accord with those described by Koski et al. (1984) for samples dredged from the same area. Their model for chimney growth differs only slightly from the one presented here; our studies indicate a minor role for anhydrite as a substrate for development of mature chimneys. The growth process is founded mainly on dendritic and colloform sphalerite, and silica. In this respect, the model for chimney construction differs significantly from those proposed for 21°N EPR that use anhydrite–sphalerite as early scaffolding (Haymon & Kastner 1981, Haymon 1983, Goldfarb et al. 1983).

EPR sulfides are very Cu-rich compared with those from southern Juan de Fuca Ridge. Nonetheless, the broad zonations of sulfates and sulfides across chimneys are much the same, differing mainly in the proportions of various minerals present and in the relative thickness of zones. Both of the chimneys studied here are irregular, and neither displays the spectacular concentric zoning seen at 21°N (Haymon & Kastner 1981).

The model for chimney growth proposed by Hannington & Scott (1988) for CASM site, Axial Seamount (a Zn-rich, Cu-poor system similar to Plume Site) is also founded on sulfate minerals (barite, anhydrite) rather than sulfides. However, chimney samples collected by submersible from the larger, active SE vent field at Axial Seamount are very similar in mineralogy and metal grades (Zn:Cu is about 25:1 with low Fe). These are currently under study (R.W. Embley, NOAA, pers. comm.).

REFERENCES

ATWATER, T. (1970): Implications of plate tectonics for the Cenozoic tectonic evolution of western North America. Geol. Soc. Amer. Bull. 81, 3513-3536.

BRETT, R., EVANS, H.T., JR., GIBSON, E.K., JR., HEDENQUIST, J.W., WANDLESS, M.V. & SOMMER, M.A. (1987): Mineralogical studies of sulfide sam-

ples and volatile concentrations of basalt glasses from the Southern Juan de Fuca Ridge. *J. Geophys. Res.* **92**, 11373-11379.

CABRI, L.J., HALL, S.R., SZYMANSKI, J.T. & STEWART, J.M. (1973): On the transformation of cubanite. *Can. Mineral.* **12**, 33-38.

DAVIS, E.E., GOODFELLOW, W.D., BORNHOLD, B.D., ADSHEAD, J.D., BLAISE, B., VILLINGER, H. & LE CHEMINANT, G.M. (1987): Massive sulfides in a sedimented rift valley, northern Juan de Fuca Ridge. *Earth Planet. Sci. Lett.* **82**, 49-61.

DIXON, J.E., CLAGUE, D.A. & EISSEN, J.P. (1986): Gabbroic xenoliths and host ferrobasalt from the southern Juan de Fuca Ridge. *J. Geophys. Res.* **91**, 3795-3820.

EMBLEY, R.W., JONASSON, I.R., PERFIT, M.R., FRANK-LIN, J.M., TIVEY, M.K., MALAHOFF, A., SMITH, M.F. & FRANCIS, T.J.G. (1988): Submersible investigation of an extinct hydrothermal system on the Galapagos Ridge: sulfide mounds, stockwork zone and differentiated lavas. *Can. Mineral.* **26**, 517-539.

GOLDFARB, M.S., CONVERSE, D.R., HOLLAND, H.D. & EDMOND, J.M. (1983): The genesis of hot spring deposits on the East Pacific Rise, 21°N. *Econ. Geol. Monogr.* **5**, 184-197.

GROSS, G.A. & McLEOD, C.R. (1988): Metallic minerals on the deep seabed. *Geol. Surv. Can. Pap.* **86-21** (with map 1659A).

HANNINGTON, M.D. & SCOTT, S.D. (1988): Mineralogy and geochemistry of a hydrothermal silica–sulfide–sulfate spire in the caldera of Axial Seamount, Juan de Fuca Ridge. *Can. Mineral.* **26**, 603-625.

———, ——— & CHASE, R.L. (1985): The Explorer Ridge polymetallic sulfide deposits: a major find in Canadian Pacific waters. Paper presented to the 16th Underwater Mining Institute, Halifax, Nova Scotia (unpubl.).

HAYMON, R.M. (1983): The growth history of hydrothermal black smoker chimneys. *Nature* **301**, 695-698.

——— & KASTNER, M. (1981): Hot spring deposits on the East Pacific Rise at 21°N; preliminary description of mineralogy and genesis. *Earth Planet. Sci. Lett.* **53**, 363-381.

HÉKINIAN, R., FEVRIER, M., BISCHOFF, J.L., PICOT, P. & SHANKS, W.C., III (1980): Sulfide deposits from the East Pacific Rise near 21°N. *Science* **207**, 1433-1444.

———, RENARD, V. & CHEMINÉE, J.L. (1984): Hydrothermal deposits on the East Pacific Rise near 13°N: Geological setting and distribution of active sulfide chimneys. *In* Hydrothermal Processes at Seafloor Spreading Centers (P.A. Rona, K. Bös-

trom, L. Laubier & K.L. Smith, Jr., eds.). Plenum Publishing Corp., New York, 571-594.

JUNIPER, S.K., THOMPSON, J.A.J. & CALVERT, S.E. (1986): Accumulation of minerals and trace elements in biogenic mucus at hydrothermal vents. *Deep-Sea Res.* **33**, 339-347.

KAPPEL, E.S. & NORMARK, W.R. (1987): Morphometric variability within the axial zone of the southern Juan de Fuca Ridge: Interpretation from Sea Marc I and deep-sea photography. *J. Geophys. Res.* **92**, 11291-11302.

KOJIMA, S. & SUGAKI, A. (1985): Phase relations in the Cu–Fe–Zn–S system between 500° and 300°C under hydrothermal conditions. *Econ. Geol.* **80**, 158-171.

KOSKI, R.A., NORMARK, W.R., MORTON, J.L. & DELANEY, J.R. (1982): Metal sulfide deposits on the Juan de Fuca Ridge. *Oceanus* **25**, 43-48.

———, CLAGUE, D.A. & OUDIN, E. (1984): Mineralogy and chemistry of massive sulfide deposits from the Juan de Fuca Ridge. *Geol. Soc. Amer. Bull.* **95**, 930-945.

LAFITTE, M., MAURY, R. & PERSEIL, E.A. (1984): Analyse minéralogique de cheminées à sulfures de la Dorsale Est Pacifique (13°N). *Minéral. Deposita* **19**, 274-282.

———, MAURY, R., PERSEIL, E.A. & BOULEGUE, J. (1985): Morphological and analytical study of hydrothermal sulfides from 21° north, East Pacific Rise. *Earth Planet. Sci. Lett.* **73**, 53-64.

LICHTMAN, G.S., NORMARK, W.R., DELANEY, J.R., MORTON, J.L. & KARSTEN, J.L. (1983): Photogeology and evolution of the Juan de Fuca Ridge. *U.S. Geol. Surv. Open-File Rep.* **83-464**.

MALAHOFF, A. (1982): A comparison of the massive submarine polymetallic sulfides of the Galapagos Rift with some continental deposits. *Mar. Tech. Soc. J.* **16**, 39-45.

MUKAIYAMA, H. & ISAWA, E. (1970): Phase relations in the Cu–Fe–S system. The copper deficient part. *In* Volcanism and Ore Genesis (T. Tatsumi, ed.). Tokyo University Press, Tokyo, 339-355.

MUROWCHICK, J.B. & BARNES, H.L. (1986): Marcasite precipitation from hydrothermal solution. *Geochim. Cosmochim. Acta* **50**, 2615-2629.

NORMARK, W.R., LUPTON, J.E., MURRAY, J.W., DELANEY, J.R., JOHNSON, H.P., KOSKI, R.A., CLAGUE, D.A. & MORTON, J.L. (1982): Polymetallic sulfide deposits and water-column of active hydrothermal vents on the southern Juan de Fuca Ridge. *Mar. Tech. Soc. J.* **16**, 46-53.

———, MORTON, J.L., KOSKI, R.A., CLAGUE, D.A. & DELANEY, J.R. (1983): Active hydrothermal vents

and sulfide deposits on the southern Juan de Fuca Ridge. *Geology* **11**, 158-163.

———, ———, HOLCOMB, R.T., KOSKI, R.A. & ROSS, S.L. (1984): A continuous linear depression in the axial valley of the southern Juan de Fuca Ridge: tectonic or volcanic origin? *Geol. Soc. Amer. Program Abstr.* **16**, 611.

———, ——— & ROSS, S.L. (1987): Submersible observations along the southern Juan de Fuca Ridge; 1984 *Alvin* program. *J. Geophys. Res.* **92**, 11283-11290.

OUDIN, E. (1983a): Hydrothermal sulfide deposits of the East Pacific Rise (21°N) Part I: descriptive mineralogy. *Mar. Geol.* **4**, 39-72.

——— (1983b): Minéralogie de gisements et indices liés à des zones d'accretion océaniques actuelles (rides Est-Pacifique et mer Rouge) et fossile (Chypre). *Chronique recherche minière* **470**, 43-55.

——— & CONSTANTINOU, G. (1984): Black smoker chimney fragments in Cyprus sulfide deposits. *Nature* **308**, 349-353.

———, PICOT, P. & POUIT, G. (1981): Comparison of sulphide deposits from the East Pacific Rise and Cyprus. *Nature* **291**, 404-407.

PHILPOTTS, J.A., ARUSCAVAGE, P.J. & VON DAMM, K.L. (1987): Uniformity and diversity in the composition of mineralizing fluids from hydrothermal vents on the southern Juan de Fuca Ridge. *J. Geophys. Res.* **92**, 11327-11333.

SCOTT, S.D. & BARNES, H.L. (1972): Sphalerite-wurtzite equilibria and stoichiometry. *Geochim. Cosmochim. Acta* **36**, 1275-1295.

——— & KISSIN, S.A. (1973): Sphalerite composition in the Zn-Fe-S system below 300°C. *Econ. Geol.* **68**, 475-479.

SHANKS, W.C.,III & SEYFRIED, W.E., JR. (1987): Stable isotope studies of vent fluids and chimney minerals, southern Juan de Fuca Ridge: Sodium metasomatism and seawater sulfate reduction. *J. Geophys. Res.* **92**, 11387-11399.

STYRT, M., BRACKMANN, A., HOLLAND, H.D., CLARKE, B., PISUTHA-ARNOND, V., ELDRIDGE, C. & OHMOTO, H. (1981): The mineralogy and the isotopic composition of sulphur in hydrothermal sulphide/sulphate deposits on the East Pacific Rise, 21°N latitude. *Earth Planet. Sci. Lett.* **53**, 382-390.

TIVEY, M.K. & DELANEY, J.R. (1986): Growth of large sulfide structures on the Endeavour Segment of the Juan de Fuca Ridge. *Earth Planet. Sci. Lett.* **77**, 303-317.

TUNNICLIFFE, V. & FONTAINE, A.R. (1987): Faunal composition and organic surface encrustations at hydrothermal vents on the southern Juan de Fuca Ridge. *J. Geophys. Res.* **92**, 11303-11314.

U.S. GEOLOGICAL SURVEY JUAN DE FUCA STUDY GROUP (1986): Submarine fissure eruptions and hydrothermal vents on the southern Juan de Fuca Ridge: Preliminary observations from the submersible *Alvin. Geology* **14**, 823-827.

VON DAMM, K.L. & BISCHOFF, J.L. (1987): Chemistry of hydrothermal solutions from the southern Juan de Fuca Ridge. *J. Geophys. Res.* **92**, 11334-11346.

WIGGINS, L.B. & CRAIG, J.R. (1980): Reconnaissance of the Cu-Fe-Zn-S system sphalerite phase relationship. *Econ. Geol.* **75**, 742-751.

YUND, R.A. & KELLERUD, G. (1966): Thermal stability of assemblages in the Cu-Fe-S system. *J. Petrology* **7**, 454-488.

ZIERENBERG, R.A., SHANKS, W.C., III & BISCHOFF, J.L. (1984): Massive sulfide deposits at 21°N, East Pacific Rise: Chemical composition, stable isotopes, and phase equilibria. *Geol. Soc. Amer. Bull.* **95**, 922-929.